

Latency Insertion Method (LIM) for the Fast Transient Simulation of Large Networks

José E. Schutt-Ainé, *Senior Member, IEEE*

Abstract—In this work, a finite difference formulation is used to simulate large networks. The method makes use or introduces reactive latency in all branches and nodes of a circuit to generate update algorithms for the voltage and current quantities. A criterion is established that guarantees the stability of the algorithm for specified choices of the time step. Because of its linear numerical complexity, several orders of magnitude in speedup over matrix-based methods are obtained. Nonlinear networks can also be simulated by the formulation. Several comparisons are made with standard simulators in order to evaluate the accuracy and efficiency of the algorithm. In all cases that satisfy the stability criterion, good agreements with established techniques are obtained.

Index Terms—Algorithm, discretization, latency, network, stability.

I. INTRODUCTION

THE need for an increased density of I/O pin connections and the reduction in size of high-speed digital circuits have led to an increase in the complexity of interconnect schemes. At the board and package levels, the implementation of multilayer interconnects has led to structures with a high density of passive components. As a result, the three-dimensional (3-D) nature of present-day networks has rendered their analysis more challenging.

These challenges are also emerging at the chip level. As outlined by the International Technology Roadmap for Semiconductors (ITRS) [1], the timeline acceleration in processor performance forecast has led to an increasing gap between manufacturing technology and present-day design tools. Total interconnect lengths will lead to unprecedented wiring density which will require novel design methodologies placing more emphasis on interconnect issues.

The simulation of very large networks consisting of large numbers of nodes is a major problem in the computer-aided design of integrated circuits. Circuits of this size can typically require several days of CPU time on a workstation. Several investigators have introduced algorithms and numerical techniques such as the asymptotic waveform evaluation (AWE) [2]–[4] method to approximate network transfer functions. The fundamental idea behind model-order reduction rests in the implementation of a circuit representation based on a smaller number of poles than the original network. These poles account for most of the behavior of the network over the frequency

range of interest. The resulting macromodel equivalent circuits can be used in conjunction with standard circuit simulators.

Work was later introduced to reduce the number of spurious poles generated by the reduction process. This includes the complex frequency hopping techniques, and the Krylov subspace methods [5]–[8]. More recent work on model order reduction techniques have focused on the passivity of the reduced equivalent circuits [9], [10].

In this study, we use a time-domain formulation that leads to the generation of update algorithms for the simulation of networks. The algorithms exhibit linear computational complexity and are scalable. Because of the time domain nature of the formulations, they can be extended to handle nonlinearities.

First, we present a formulation of the method for the case of linear networks by deriving the update algorithms. Next, the stability of these algorithms is addressed followed by an extension of the formulation to special elements and nonlinear networks. Finally, several networks are analyzed and simulated using the method for comparison with standard simulators. Tradeoffs between speed, stability, and accuracy are examined throughout the comparisons.

II. FORMULATION FOR LINEAR NETWORKS

Distributed networks are often used to describe signal propagation on uniform transmission lines (Fig. 1). This model is also a high-frequency representation of an interconnection. Fig. 2 shows a more general interconnection topology in which signals can propagate in more than one direction. Such a model can be viewed as the high-frequency representation of an arbitrary network. In analyzing an arbitrary network, we can define a branch as a connection between two nodes (excluding the ground reference node). In defining the desired topology for such an analysis, the following requirements are made.

- 1) Each branch of the network must contain an inductance; otherwise, a small inductance is inserted into the branch to generate the latency.
- 2) Each node of the network must provide a capacitive path to ground; otherwise, a small shunt capacitor is added to generate latency at that node.

In addition, it is also assumed that by using combinations of Thévenin and Norton transformations, all branches and nodes can be converted to this topology. After all augmentations and reductions are performed, network branches are represented with a voltage source, a resistor, and an inductor in series. All connections to ground are represented by a parallel combination

Manuscript received October 25, 1999; revised April 20, 2000. This paper was recommended by Associate Editor Y. Park.

The author is with the Department of Electrical and Computer Engineering, University of Illinois, Urbana, IL 61801 USA.

Publisher Item Identifier S 1057-7122(01)00660-2.

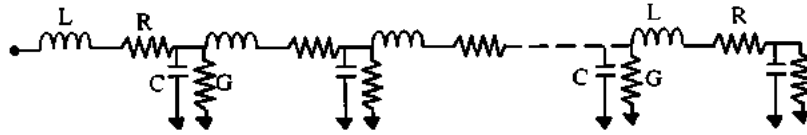


Fig. 1. Discrete distributed model for uniform transmission line. R , L , G , and C are the resistance, inductance, conductance, and capacitance per unit length, respectively.

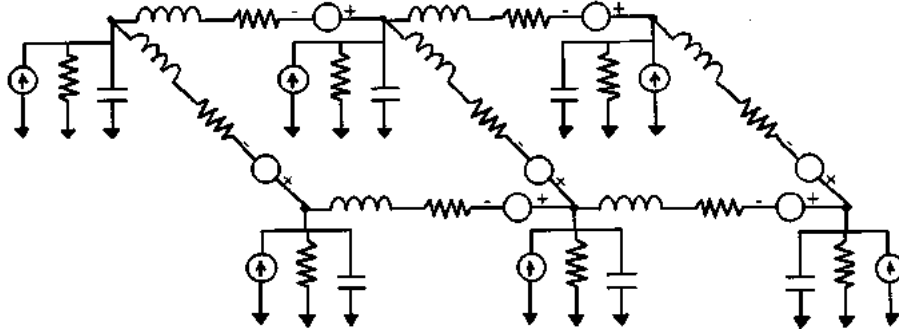


Fig. 2. Network with interconnect topology.

of a current source, a capacitance, and a conductance to ground from every node.

First, the time variable is discretized, next the voltage and current quantities are collocated in half time steps to generate sequences of the form $V^{n-1/2}$, $V^{n+1/2}$, $V^{n+3/2}$ for voltages and I^n , I^{n+1} , I^{n+2} for currents.

A. Branch Algorithm

Each branch is represented as a combination of a voltage source, an inductor, and a resistor in series. Current I_{ij} is assumed to be directed from node i at voltage V_i to node j at potential V_j (see Fig. 3).

The discrete time equation reads

$$\begin{aligned} V_i^{n+1/2} - V_j^{n+1/2} \\ = L_{ij} \left(\frac{I_{ij}^{n+1} - I_{ij}^n}{\Delta t} \right) + R_{ij} I_{ij}^n - E_{ij}^{n+1/2}. \end{aligned} \quad (1)$$

Solving for the unknown current leads to

$$I_{ij}^{n+1} = I_{ij}^n + \frac{\Delta t}{L_{ij}} \left(V_i^{n+1/2} - V_j^{n+1/2} - R_{ij} I_{ij}^n + E_{ij}^{n+1/2} \right). \quad (2)$$

At each time step, this operation is performed over all N_b branches of the network in order to update all the current values.

B. Node Algorithm

Each node is modeled as a parallel combination of a current source, a conductance, and a capacitor to ground as shown in Fig. 4. The equation reads

$$C_i \left(\frac{V_i^{n+1/2} - V_i^{n-1/2}}{\Delta t} \right) + G_i V_i^{n+1/2} - H_i^n = - \sum_{k=1}^{M_i} I_{ik}^n \quad (3)$$

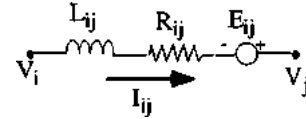


Fig. 3. Branch equation formulation.

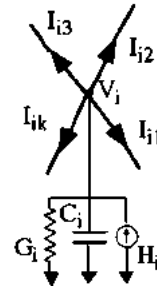


Fig. 4. Node equation formulation.

where M_i is the number of branches connected to node i (excluding connections to ground). This yields

$$V_i^{n+1/2} = \frac{\frac{C_i V_i^{n-1/2}}{\Delta t} + H_i^n - \sum_{k=1}^{M_i} I_{ik}^n}{\frac{C_i}{\Delta t} + G_i} \quad (4)$$

for $i = 1, 2, \dots, N_n$. At each time step, this operation is performed over all N_n nodes in order to update all the voltage quantities.

Computations of all branch currents then all node voltages are alternated as time progresses; thus a complete network simulation can be summarized by the following algorithm.

For time=1, N_t
 For branch=1, N_b
 Update current as per (2);
 Next branch;
 For node=1, N_n

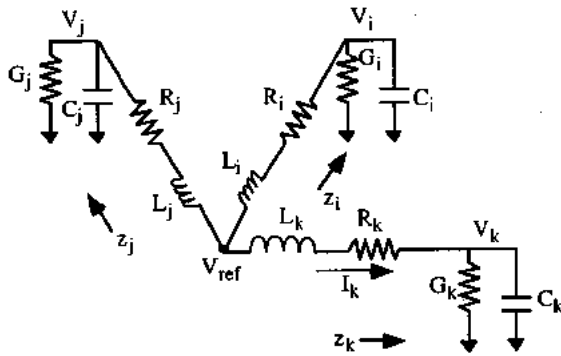


Fig. 5. Multidirectional network.

Update voltage as per (4);
Next node;
Next time;

Altogether, $N_t(N_n + N_b)$ operations are performed to obtain $N_t(N_n + N_b)$ values, hence yielding an optimally efficient algorithm.

III. STABILITY CONSIDERATIONS

A numerical stability analysis of the latency insertion method (LIM) is now performed to establish the relationship between the time steps and the parameters of the network. From a wave point of view, because of the nonisotropic nature of the discrete network, a signal propagates with different speeds in different directions. If a node is chosen as the reference and voltage variations at another node are observed, propagation in one direction can be analyzed through the use of the Telegrapher's Equations. In the discrete domain, choosing the z_k direction as shown in Fig. 5, the formulation reads

$$-\frac{\Delta_f V_k}{\Delta z_k} = L_k \frac{\Delta_f I_k}{\Delta t} + R_k I_k \quad (5a)$$

$$-\frac{\Delta_b I_k}{\Delta z_k} = C_k \frac{\Delta_b V_k}{\Delta t} + G_k V_k \quad (5b)$$

where Δ_f and Δ_b refer to the forward and backward differential operators, respectively. First, in the case where R_k and G_k are negligible, numerical stability at node k will be achieved if for an oscillatory response in the time domain, the resulting signal propagating in the z_k direction is attenuated. If we assume a dependence in the form of the discrete oscillator [11], the associated condition is

$$\Delta z_k > \frac{\Delta t}{\sqrt{L_k C_k}} \quad (6)$$

which is analogous to the Courant–Friedrichs–Lewy (CFL) criterion for wave propagation in a discrete grid [12]. This condition is still valid when R_k and G_k are nonzero. When translated to a per cell basis, the relation becomes

$$\Delta t < \sqrt{L_k C_k}. \quad (7)$$

This inequality can be viewed as a causality condition in tracking a propagating signal through a lattice of circuit elements. The condition imposes some constraints that may limit

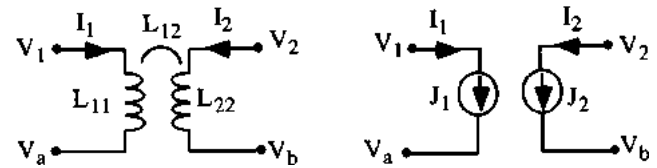
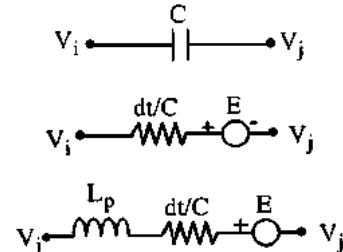


Fig. 6. Derivation of LIM equivalent circuit for mutual inductance; left: original representation, right: equivalent circuit.

Fig. 7. Derivation of LIM equivalent circuit for branch capacitor. First, backward Euler companion model is built; next, latency is introduced through L_p .

the numerical efficiency of the method for large networks with low latency. For such networks, insertion of small reactive elements lead to smaller time steps from (7) leading to longer simulations.

IV. NETWORK REDUCTION OF SPECIAL ELEMENTS

The LIM formulation is based on branch or node topology requirements that are not met by some circuit elements. Those elements can be transformed through reduction or augmentation before they can be incorporated in the formulation. These include mutual inductance, branch capacitance, and controlled sources. The transformation is performed by insertion of a delay and by representation with the numerical integration-based companion models [13]. For the coupled inductor system shown in Fig. 6, a transformation must be performed to an equivalent circuit that will represent the combined effect of the self- and mutual inductances. The system satisfies the matrix relation

$$\mathbf{V} = \mathbf{L} \frac{\partial \mathbf{I}}{\partial t} \quad (8)$$

where

$$\mathbf{V} = \begin{bmatrix} V_1 - V_a \\ V_2 - V_b \end{bmatrix}, \quad \mathbf{I} = \begin{bmatrix} I_1 \\ I_2 \end{bmatrix}$$

and

$$\mathbf{L} = \begin{bmatrix} L_{11} & L_{12} \\ L_{21} & L_{22} \end{bmatrix}. \quad (9)$$

In the discrete domain

$$\mathbf{V} = \mathbf{L} \frac{\Delta \mathbf{I}}{\Delta t} \quad (10)$$

or

$$\frac{\Delta \mathbf{I}}{\Delta t} = \mathbf{L}^{-1} \mathbf{V}. \quad (11)$$

Using the forward Euler numerical integration formula

$$\mathbf{I}^{n+1} = \mathbf{I}^n + \delta \mathbf{I}^n \quad (12)$$

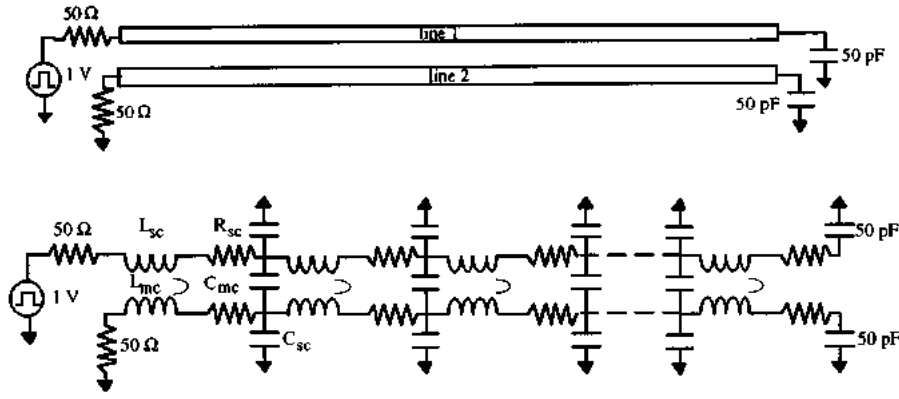


Fig. 8. Top: coupled line structure with capacitive terminations. The electrical parameters are $L_s = 455$ nH/m, $C_s = 77$ pF/m, $L_m = 147$ nH/m, and $C_m = 22$ pF/m. The length of the lines is $d = 14$ in. Bottom: discrete distributed model used to represent the transmission line system. The number of cells is $N = 50$. The cell element values are: $L_{sc} = dL_s/N$, $L_{mc} = dL_m/N$, $C_{sc} = dC_s/N$, $C_{mc} = dC_m/N$, $R_{sc} = 0$ Ω .

where δ is the time step and $I^{n'}$ is the time derivative of I^n . Using (11) as the discrete derivative and expanding, we get

$$I_1^{n+1} = I_1^n + \delta g_{11}(V_1 - V_a) + \delta g_{12}(V_2 - V_b) \quad (13a)$$

$$I_2^{n+1} = I_2^n + \delta g_{21}(V_1 - V_a) + \delta g_{22}(V_2 - V_b) \quad (13b)$$

more explicitly and using $\delta = \Delta t$

$$I_1^{n+1} = I_1^n + g_{11} \left(V_1^{n+1/2} - V_a^{n+1/2} \right) \Delta t + g_{12} \left(V_2^{n+1/2} - V_b^{n+1/2} \right) \Delta t = J_1 \quad (14a)$$

$$I_2^{n+1} = I_2^n + g_{21} \left(V_1^{n+1/2} - V_a^{n+1/2} \right) \Delta t + g_{22} \left(V_2^{n+1/2} - V_b^{n+1/2} \right) \Delta t = J_2 \quad (14b)$$

where

$$g_{11} = \frac{L_{22}}{L_{11}L_{22} - L_{12}L_{21}} \quad (15a)$$

$$g_{21} = \frac{-L_{21}}{L_{11}L_{22} - L_{12}L_{21}}$$

$$g_{12} = \frac{-L_{12}}{L_{11}L_{22} - L_{12}L_{21}}$$

$$g_{22} = \frac{L_{11}}{L_{11}L_{22} - L_{12}L_{21}}. \quad (15b)$$

The system can be represented by the equivalent circuit shown in Fig. 6, in which the current sources J_1 and J_2 depend on the history of the coupled system. After this transformation, the resulting branches can be easily inserted into an existing network. In a similar manner, branch capacitors can be transformed and represented by their discrete numerical integration companion models [13] (see Fig. 7). In order to generate the latency, a small inductor is inserted within the branch. Similar transformations can be performed for other elements including inductors to ground.

In order to validate these transformation methods and assess the accuracy of the resulting algorithms, computer simulations and laboratory experiments were performed and compared. For the experimental setup, a coupled microstrip system was designed and terminated as shown in Fig. 8. One line was used as a drive line and excited with a 12-ns-wide pulse; the adjacent

line was used as a sense line. Voltage responses were measured at the near ends of both drive and sense lines. For the computer simulation, the discrete distributed model for coupled transmission lines shown in Fig. 8 was used. The system consisted of 50 cells. Mutual inductors and capacitors were modeled using the method described above. Fig. 9 shows the waveforms obtained for both experimental and computer simulations. Good agreement was obtained for both drive and sense line responses.

V. NONLINEAR FORMULATION

One advantage of time-domain formulations for circuit analysis rests on the ability to handle nonlinear behaviors. In addition to interconnects, most integrated circuits contain a large number of nonlinear devices such as diodes and transistors. When the number of these elements becomes large, matrix-based methods become inefficient. Since the latency insertion method uses a time-domain formulation, the extension to nonlinearities is straightforward. For such devices, the current-voltage relation is expressed through a nonlinear function. Without loss of generality, such current-voltage relation can be expressed as: $i = f(v)$ such that $v = f^{-1}(i)$, where f^{-1} is the associated inverse function (Fig. 10). In a similar manner as in the linear case, the branch and the node formulations are separated.

When the nonlinear element is inserted into a branch with latency (see Fig. 11), the discretized formulation becomes

$$V_i^{n+1/2} - V_j^{n+1/2} = L_{ij} \left(\frac{I_{ij}^{n+1} - I_{ij}^n}{\Delta t} \right) + R_{ij} I_{ij}^{n+1} - E_{ij}^{n+1/2} + f^{-1}(I_{ij}^{n+1}). \quad (16)$$

The unknown current I_{ij}^{n+1} can be solved by iteration using the Newton-Raphson algorithm. When the variables I_{ij}^{n+1} and $f^{-1}(I_{ij}^{n+1})$ are replaced by X and V , respectively, the iteration formula for the current solution becomes

$$X^{(k+1)} = X^{(k)} - \frac{L_{ij} [X^{(k)} - I_{ij}^n] + R_{ij} X^{(k)} + H + V}{\frac{L_{ij}}{\Delta t} + R_{ij} + \frac{\partial V}{\partial X}} \quad (17)$$

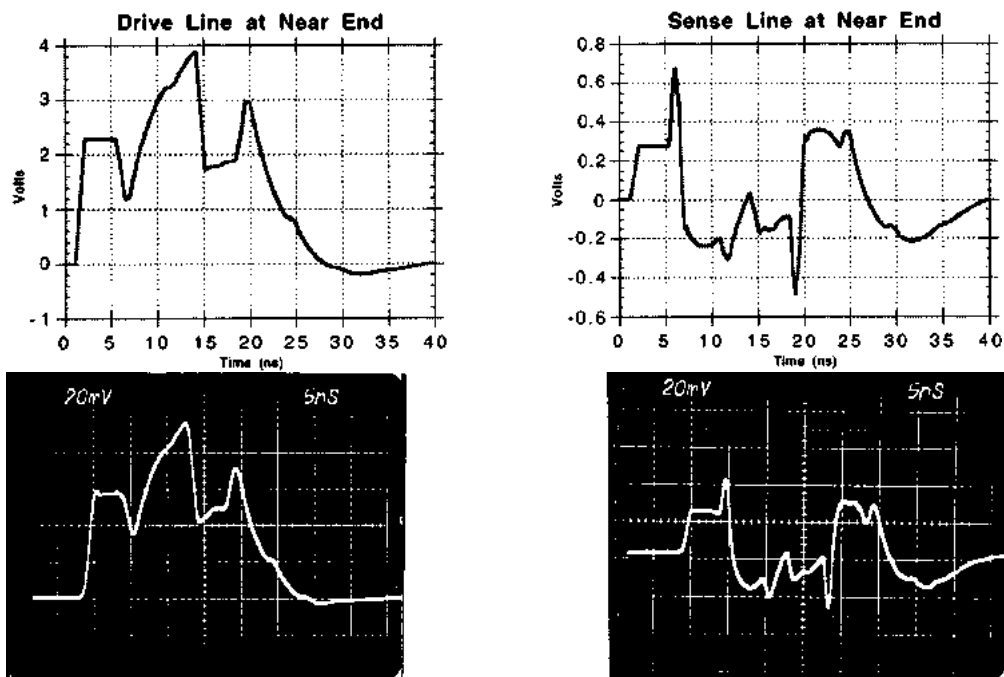


Fig. 9. Computer simulations of distributed model (top) and experimental waveforms of coupled microstrip lines (bottom) for the circuit of Fig. 8 at the near end ($x = 0$) for line 1 (left) and line 2 (right). The pulse characteristics are magnitude = 4 V; width = 12 ns; rise and fall times = 1 ns. The photograph probe attenuation factors are 40 (left) and 10 (right).

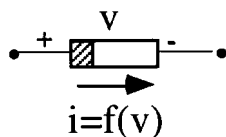


Fig. 10. Nonlinear element.

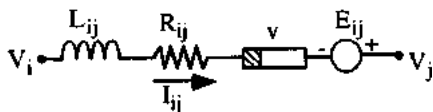


Fig. 11. Nonlinear branch equation formulation.

where $H = V_j^{n+1/2} - V_i^{n+1/2} - E_{ij}^{n+1/2}$. The subscript (k) refers to the k th iteration. These are performed on the branch under consideration at a given time step.

In the case where a nonlinear element provides a path to ground, the network with latency, shown in Fig. 12, is used. The discretized equation reads

$$C_i \left[\frac{V_i^{n+1/2} - V_i^{n-1/2}}{\Delta t} \right] + G_i V_i^{n+1/2} - H_i^n + f(V_i^{n+1/2}) = - \sum_{k=1}^{M_i} I_{ik}^n. \quad (18)$$

The voltage $V_i^{n+1/2}$ can be solved iteratively using the Newton–Raphson algorithm. Replacing $V_i^{n+1/2}$ and

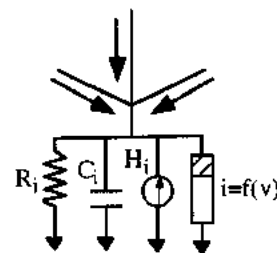


Fig. 12. Nonlinear node equation formulation.

$f(V_i^{n+1/2})$ with X and I , respectively, the iteration algorithm becomes

$$X^{(k+1)} = X^{(k)} - \frac{X^{(k)} \left[\frac{C_i}{\Delta t} + G_i \right] - H_i + \sum_{k=1}^{M_i} I_{ik}^n + I}{\left[\frac{C_i}{\Delta t} + G_i \right] + \frac{\partial I}{\partial X}}. \quad (19)$$

The iteration is performed until convergence to the node voltage solution. It must be emphasized that in both branch and node cases, the iterations are performed only on the branches and nodes containing the nonlinear elements. This leads to a significant computational advantage over standard modified nodal analysis (MNA) methods in which the iterations are performed over the entire network consisting of both linear and nonlinear components.

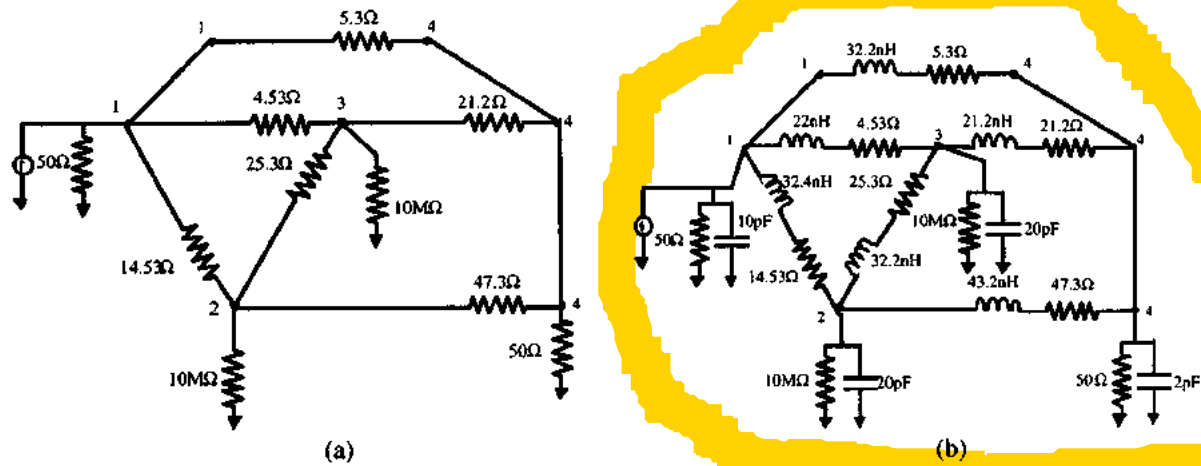


Fig. 13. (a) Network with zero latency to be simulated. (b) Augmented network used for simulation with LIM. The base values are shown for the inductive and capacitive elements. For each simulation, these values are divided by a scaling factor to approximate the response of the circuit in (a).

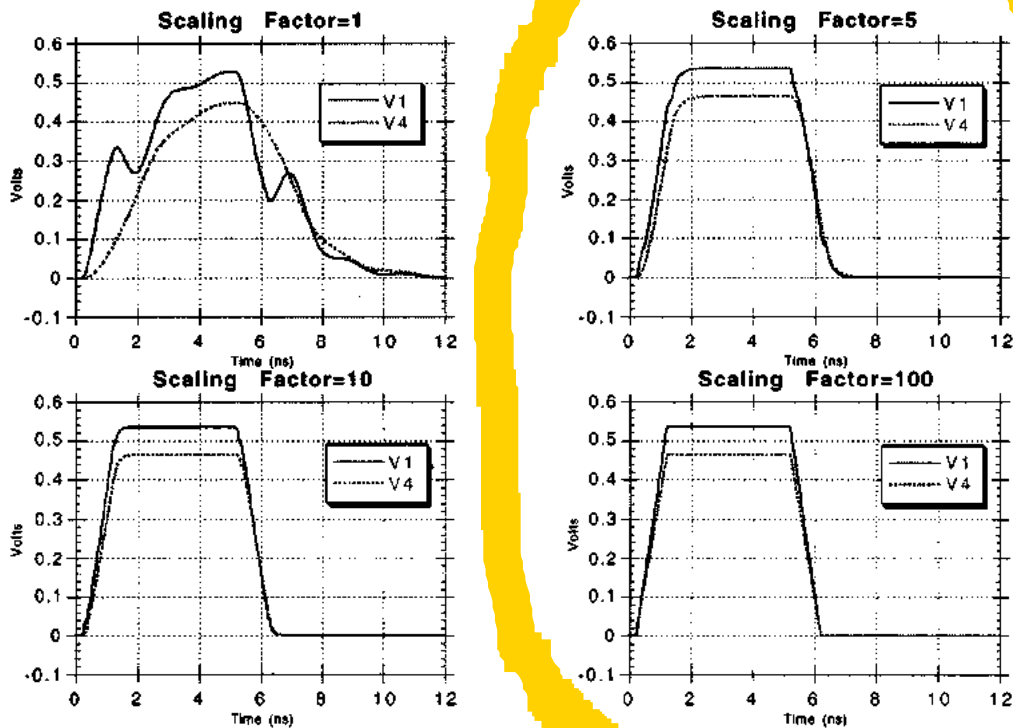


Fig. 14. Simulation results for various levels of scaling of the reactive elements of the network of Fig. 13(b) to emulate the actual response of the network in Fig. 13(a). Response waveforms shown are for nodes 1 and 4. Inductive and capacitive elements of Fig. 13(a) are divided by the scaling factor.

The complete nonlinear network simulation is thus summarized by the following algorithm:

```

For time=1,  $N_t$ 
  For branch=1,  $N_b$ 
    If branch is linear
      Update current as per (2);
    Else
      Iterate and update current as per (17);
    Next branch;
  For node=1,  $N_n$ 
    If node is linear
      Update voltage as per (4);

```

Else

```

  Iterate and update voltage as per (19);
  Next node;
Next time;

```

Generalization of this algorithm to networks with transistors (e.g., MOSFET, BJT) follows naturally from the previous developments. In particular, when inverse functions relating voltage and current variables cannot be extracted analytically, nonlinear devices can be represented by their linearized Newton–Raphson equivalent circuits at each iteration [13]. The derivation and illustration of these schemes are outside the scope of the present work and will be the subject of a future paper.

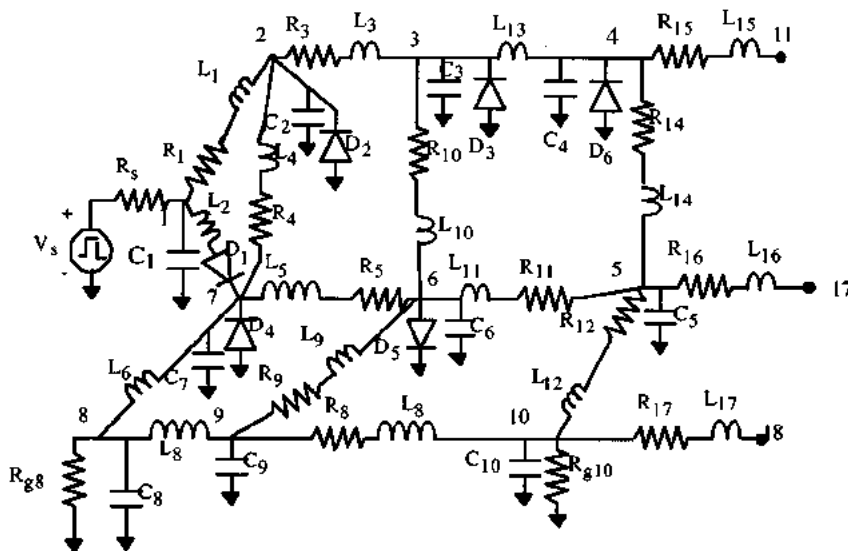


Fig. 15. Nonlinear circuit used for computer simulations.

TABLE I
ELEMENT VALUES FOR TEST CIRCUIT OF FIG. 15

Inductance (nH)	Capacitance (pF)	Resistance (Ω)	Diode Parameters
$L_1=42.8$	$C_1=9.2$	$R_1=65$	Saturation current: $I_s = 10^{-15}$ A Thermal voltage: $V_T = 0.026$ V
$L_2=0.25$	$C_2=0.1$	$R_3=10$	
$L_3=0.25$	$C_3=9.8$	$R_4=100$	
$L_4=0.25$	$C_4=0.1$	$R_5=30$	
$L_5=42.7$	$C_5=7.8$	$R_8=100$	
$L_6=109$	$C_6=0.1$	$R_9=47$	
$L_7=209$	$C_7=17.8$	$R_{10}=100$	
$L_8=0.25$	$C_8=4.8$	$R_{11}=25$	
$L_9=0.25$	$C_9=8.9$	$R_{12}=40$	
$L_{10}=0.25$	$C_{10}=0.1$	$R_{14}=30$	
$L_{11}=0.25$		$R_{15}=5$	
$L_{12}=36.6$		$R_{16}=2$	
$L_{13}=10$		$R_{17}=8$	
$L_{14}=0.25$		$R_3=50$	
$L_{15}=30$		$R_{g8}=100$	
$L_{16}=20$		$R_{g10}=100$	
$L_{17}=40$			

VI. LATENCY SIMULATIONS

Worst case analysis of the LIM can be performed by analyzing networks with low latency. Such a network is shown in Fig. 13(a). In order to simulate its transient response using a LIM approach, the augmented network of Fig. 13(b) is implemented. Base values are first chosen for the reactive elements. These base values are then divided by a scaling factor before each simulation with larger scaling factors corresponding to better approximations of the actual transient response of the circuit in Fig. 13(a).

Simulations were performed for scaling factors of 1, 5, 10, and 100. The excitation was a pulse with rise and fall times of 1 ns and pulse width of 4 ns. The resulting transient response waveforms are shown in Fig. 14. As expected, a sufficiently accurate response can be obtained; however, this also requires a

scaling of the time step leading to a reduction in computational speed. This compromise is a consequence of the stability condition (7) and is also a strong function of the excitation used in the transient simulation.

VII. NONLINEAR AND LARGE NETWORK SIMULATIONS

As a first step, the accuracy of the method at estimating transients in nonlinear networks is evaluated. For this purpose, the basic linear network shown in Fig. 15 is analyzed. The network consists of resistive, reactive, and nonlinear elements. Actual values used in the simulations are shown in Table I. The nonlinear elements are diodes which obey the well known equation

$$I_D = I_S(e^{V_D/V_T} - 1) \quad (20)$$

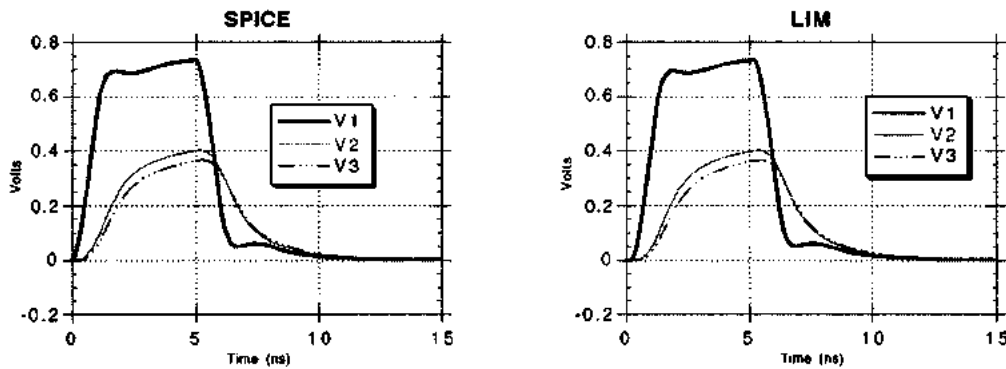


Fig. 16. Plots of waveform for nonlinear circuit for SPICE (left) and LIM (right). The pulse characteristics for V_s are: magnitude = 1 V, rise and fall times = 1 ns, pulsewidth = 4 ns.

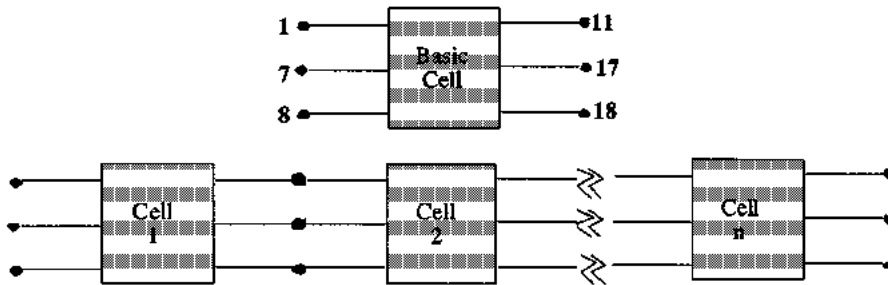


Fig. 17. Top: Basic cell used for nonlinear analysis. Numbers refer to nodes of circuit in Fig. 15. Bottom: Cell arrangement for large network analysis.

where I_D and V_D are the diode current and voltage, respectively, I_S is the saturation current, and V_T the thermal voltage. The inverse function associated with this nonlinear behavior is

$$V_D = V_T \ln \left(\frac{I_D}{I_S} + 1 \right). \quad (21)$$

The analytical expressions for the derivatives of these functions, as required by the iteration algorithms (17) and (19), can be easily obtained. Both voltage and current iterations are used in the solution process; moreover, when the bias voltage across the diodes is below a threshold value, a linear model for the I - V relation is used [14].

The network which is defined as a basic cell is excited with a pulse. The resulting waveforms are simulated using both SPICE and the proposed formulation. Plots of the waveforms are shown in Fig. 16. They indicate a good agreement between the two methods.

Next, larger networks are constructed by cascading segments of the basic cell network totaling in larger numbers of nodes and branches (Fig. 17). A pulse with shorter duration is used for the excitation. Simulations are performed again using SPICE and the proposed method for 100 time steps. Table II shows the computational performance comparison between the two methods. Several orders of magnitude are gained through the use of the LIM approach.

VIII. REMARKS AND OBSERVATIONS

Since the LIM formulation introduces latency, it is a high-frequency method that approximates an arbitrary network as a multidirectional interconnect with inductance in every branch

TABLE II
COMPARISON OF RUN TIMES

Number of Nodes	SPICE (sec)	LIM (sec)
1,000	9	0.25
10,000	334	4
15,000	701	6
20,000	1224	9
25,000	1892	11
30,000	2935	13

and shunt capacitance at every node. The method is the circuit analog of the finite difference time domain (FDTD) method. Based on the Yee algorithm [15], the FDTD method generates field solutions in time and space from the update equations. Although the FDTD method can be very intensive, it is an optimally efficient algorithm [16] and has linear computational complexity. Scalar formulations of the FDTD method have been used to analyze uniform transmission lines [17]. The present method can thus be viewed as a generalization that introduces nonuniformity and multidimensionality in the transmission lines. Accuracy, stability and efficiency of the LIM method are increased for higher frequency or faster signals which justifies its characterization as a high-frequency simulation method.

IX. CONCLUSION

An efficient method for the simulation of large networks has been presented. The method introduces or uses latency behavior in the network to generate update equations for the branch currents and node voltages. First simulation algorithms were derived for linear passive networks; the formulation was then extended to handle nonlinear elements. Comparisons with SPICE have shown speedups of several orders of magnitude.

ACKNOWLEDGMENT

The author wishes to thank Prof. I. N. Hajj for valuable comments and suggestions during the development of this work.

REFERENCES

- [1] International Technology Roadmap for Semiconductors. (1999). [Online]. Available: <http://notes.sematech.org/1999SIARoadmap/Home.htm>
- [2] L. T. Pillage and R. A. Rohrer, "Asymptotic waveform evaluation for timing analysis," *IEEE Trans. Computer-Aided Design*, vol. 9, pp. 352–366, Apr. 1990.
- [3] J. Bracken, V. Raghavan, and R. Rohrer, "Interconnect simulation with asymptotic waveform evaluation (AWE)," *IEEE Trans. Circuits Syst.*, vol. 39, pp. 869–878, Nov. 1992.
- [4] T. Tang and M. Nakhla, "Analysis of lossy multiconductor transmission lines using the asymptotic waveform evaluation technique," *IEEE Trans. Microwave Theory Tech.*, vol. 39, pp. 2107–2116, Dec. 1991.
- [5] E. Chiprout and M. S. Nakhla, "Analysis of interconnect networks using complex frequency hopping (CFH)," *IEEE Trans. Computer-Aided Design*, pp. 186–200, Feb. 1995.
- [6] P. Feldmann and R. W. Freund, "Efficient linear cut analysis by Padé via Lanczos process," *IEEE Trans. Computer-Aided Design*, vol. 14, pp. 639–649, May 1995.
- [7] M. Celik and A. Cangellaris, "Simulation of dispersive multiconductor transmission lines by Padé approximation via Lanczos process," *IEEE Trans. Microwave Theory Tech.*, vol. 44, pp. 2525–2535, Dec. 1996.
- [8] W. T. Beyene and J. E. Schutt-Ainé, "Accurate frequency-domain modeling and efficient circuit simulation of high-speed package interconnects," *IEEE Trans. Microwave Theory Tech.*, vol. 45, pp. 1941–1947, Oct. 1997.
- [9] A. Odabasioglu, M. Celik, and L. Pillegi, "PRIMA: Passive reduced-order interconnect macromodeling algorithm," in *Proc. Int. Conf. Computer-Aided Design-97*, Nov. 1997, pp. 58–65.
- [10] Q. Yu, J. Wang, and E. Kuh, "Passive multipoint moment matching model order reduction algorithm on multipoint distributed interconnect networks," *IEEE Trans. Circuit Syst.*, vol. 46, pp. 140–160, Jan. 1999.
- [11] J. E. Schutt-Ainé, "Analysis of FDTD method via the discrete oscillator," in *1999 IEEE Antenna Propagation Symp.*, Orlando, FL.
- [12] R. Courant, K. O. Friedrichs, and H. Lewy, "Über die Partiaellen Differenzengleichungen der Mathematischen Physik," *Math. Ann.*, vol. 100, no. 32, 1928.
- [13] L. O. Chua and P. M. Lin, *Computer-Aided Analysis of Electronic Circuits*. Englewood Cliffs, NJ: Prentice-Hall, 1975.
- [14] J. Vlach and K. Singhal, *Computer Methods for Circuit Analysis*, 2nd ed. New York: Chapman and Hall, 1997.
- [15] K. S. Yee, "Numerical solution of initial boundary value problems involving Maxwell's equations in isotropic media," *IEEE Trans. Antennas Propagat.*, vol. 14, pp. 302–307, May 1966.
- [16] W. C. Chew and W. H. Weedon, "A 3D perfectly matched medium from modified Maxwell's equations with stretched coordinates," *Micro. Opt. Tech. Lett.*, vol. 7, pp. 599–604, Sept. 1994.
- [17] C. R. Paul, "Incorporation of terminal constraints in the FDTD analysis of transmission lines," *IEEE Trans. Electromagn. Compat.*, vol. 36, pp. 85–91, May 1994.



José E. Schutt-Ainé (S'87–M'88–SM'98) received the B.S. degree from the Massachusetts Institute of Technology, Cambridge, MA, and the M.S. and Ph.D. degrees from the University of Illinois, Urbana Champaign, in 1984 and 1988, respectively.

He started his career as an Application Engineer at the Hewlett-Packard Microwave Technology Center in Santa Rosa, CA, during 1981–1983 and was involved in the design and testing of high frequency. His work also included the modeling and testing of microwave bipolar transistors. He has held positions at GTE Network Systems in Northlake, IL, and Digital Equipment Corp. in Hudson, MA, where he conducted research in signal integrity in high-speed digital telecommunication networks and computer-aided design tool development. He joined the faculty of the Electromagnetic Communication Laboratory, University of Illinois, in 1989 where he is currently Associate Professor of Electrical and Computer Engineering. Prof. Schutt-Ainé's interests include microwave theory and measurements, electromagnetics, high-speed digital circuits, solid-state electronics, and the design and simulation of electronic packages.